Microwave photon generation in a doubly tunable superconducting resonator

IOP Conf. Series: Journal of Physics: Conf. Series **969** (2018) 012146 doi:10.1088/1742-6596/969/1/012146

Microwave photon generation in a doubly tunable superconducting resonator

I-M. Svensson[1], M. Pierre, M. Simoen, W. Wustmann, P. Krantz, A. Bengtsson, G. Johansson, J. Bylander, V. Shumeiko and P. Delsing

Microtechnology and Nanoscience, Chalmers University of Technology, Göteborg, Sweden

E-mail: [1]ida-maria.svensson@chalmers.se

Abstract. We have created a doubly tunable resonator, with the intention to simulate relativistic motion of the resonator boundaries in real space. Our device is a superconducting coplanar-waveguide microwave resonator, with fundamental resonant frequency $\omega_1/(2\pi) \sim 5\,\mathrm{GHz}$. Both of its ends are terminated to ground via dc-SQUIDs, which serve as magnetic-flux-controlled inductances. Applying a flux to either SQUID allows the tuning of $\omega_1/(2\pi)$ by approximately 700 MHz. Using two separate on-chip magnetic-flux lines, we modulate the SQUIDs with two tones of equal frequency, close to $2\omega_1$. We observe photon generation, at ω_1, above a certain pump amplitude threshold. By varying the relative phase of the two pumps we are able to control this threshold, in good agreement with a theoretical model. At the same time, some of our observations deviate from the theoretical predictions, which we attribute to parasitic couplings resulting in current driving of the SQUIDs.

1. Introduction

Vacuum is commonly considered to be empty space. However, in quantum theory, it contains vacuum fluctuations of the electromagnetic field. Due to these fluctuations, two perfectly conducting mirrors at rest, placed in close vicinity of each other, can exhibit radiation pressure forces, known as the Casimir effect [1]. Furthermore, if the mirrors are moved with a speed close to the speed of light, real photons can be generated as excitations of the vacuum fluctuations, a phenomenon called the dynamical Casimir effect (DCE) [2]. In fact, photon generation through the DCE requires only one rapidly moving mirror to produce photons [3, 4].

Using superconducting circuits, the physical conditions equivalent to a mirror moving at about 1/4 of the speed of light can be created [5]. This is done by placing a superconducting quantum interference device (SQUID) at the end of a transmission line. The SQUID acts as a tunable inductance, $L_J(\Phi_{ext}, I_s) = \Phi_0/\left(2\pi|\cos(\Phi_{ext}\pi/\Phi_0)|\sqrt{I_c^2 - I_s^2}\right)$, where Φ_0 is the magnetic flux quantum, $\Phi_{ext} = \Phi_{dc} + \Phi_{ac}(t)$ is the applied external magnetic flux, I_c is the SQUID's critical current, and I_s the current through the SQUID. The SQUID inductance can be modulated either by flux pumping, through Φ_{ac}, which is a direct modulation of the resonator boundary condition and the analogue of a moving mirror, or by ac driving the SQUID current I_s. The generation of DCE photons using a flux-pumped SQUID at the end of a transmission line was suggested in Ref. [6] and demonstrated in Ref. [7].

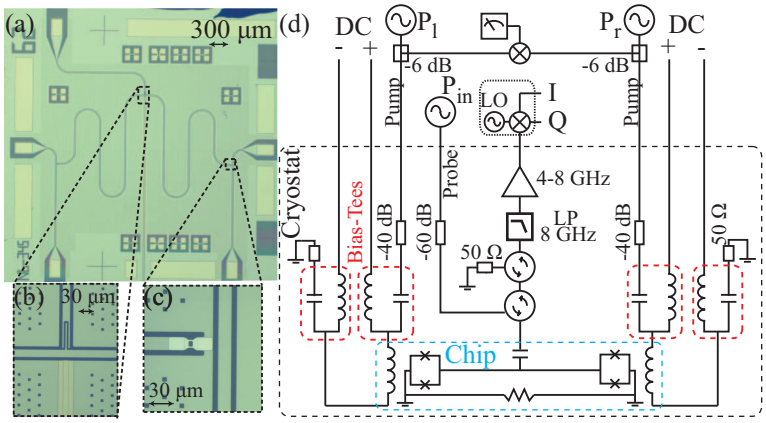

Figure 1. (a) Micrograph of the doubly tunable resonator chip. (b) Resonator middle with a gold-filled slot (below) and a coupling capacitor and probe (above). (c) Resonator end with the SQUID and on-chip flux line. (d) Schematic of the measurement setup. It is a reflection setup with circulators to probe the resonant frequency and also to measure the output when the resonator is pumped through the on-chip flux lines.

If a SQUID is included in a resonator and flux-modulated around twice the resonant frequency, the system is the equivalent of a parametric oscillator (PO) [8–10], *i.e.* a harmonic oscillator driven by the modulation of a system parameter, here the resonant frequency. The PO has a flux-pump amplitude threshold, determined by the system damping,above which self-sustained oscillations are generated [9]. Below threshold, the system can be operated as a parametric amplifier in which small input signals near its resonant frequency are amplified [11–14].

In this paper we use a superconducting coplanar waveguide $\lambda/2$ resonator, with each end grounded via a SQUID. If driven separately, both SQUIDs can generate photons individually through the DCE. When driven together at the same frequency, the resonator can be thought of as a vibrating resonator or a breathing resonator, depending on the phase difference between the two drive signals. When flux pumping both SQUIDs around $2\omega_1$, theory predicts constructive interference for the breathing mode, leading to a low threshold for photon generation, and destructive interference for the vibrating mode, *i.e.* no photon generation [15–19]. In addition to investigations of the DCE this device opens up doors for future interesting experiments, for example, measurements of the twin paradox [20], where a microwave signal could be sent on a "space trip" in a vibrating resonator, and the generation of cluster states [21].

2. Experimental setup

Our circuit is placed on a sapphire substrate (Fig. 1). The SQUIDs are made of aluminium and deposited by two-angle evaporation, while the rest of the circuit is etched in niobium. The resonator is meandered and grounded in both ends. To avoid a parasitic superconducting loop through resonator and ground plane, we made a slot in the ground plane. To keep good electrical contact we bridged the slot with normal metal (gold), see Fig. 1(b).

We use a reflection setup with circulators to allow for proper attenuation of an input probe signal and amplification of the resonator output signal (Fig. 1(d)). The flux-line setup enable both dc biasing and fast modulation (pumping) through separate lines that are combined in bias-Tees at the mixing chamber stage of the cryostat. The pump signals are generated in two sources, $P_{l/r}$, phase locked by a 10 MHz reference. To measure the phase difference between the sources, their output signals are divided in power splitters and compared using a mixer. Provided that the two pumps have the same frequency, the mixer output is a dc voltage with varying amplitude, depending on the phase difference between the pumps. The resonator output is down-converted and sampled in a digitizer, which records both the in- and out-of-phase quadratures.

3. Measurement results - Resonator characterization

We tune the resonant frequency by controlling the two dc-fluxes, $\Phi_{dc,l/r}$. The first resonator mode is probed by measuring the reflection coefficient of a microwave signal incident on the resonator

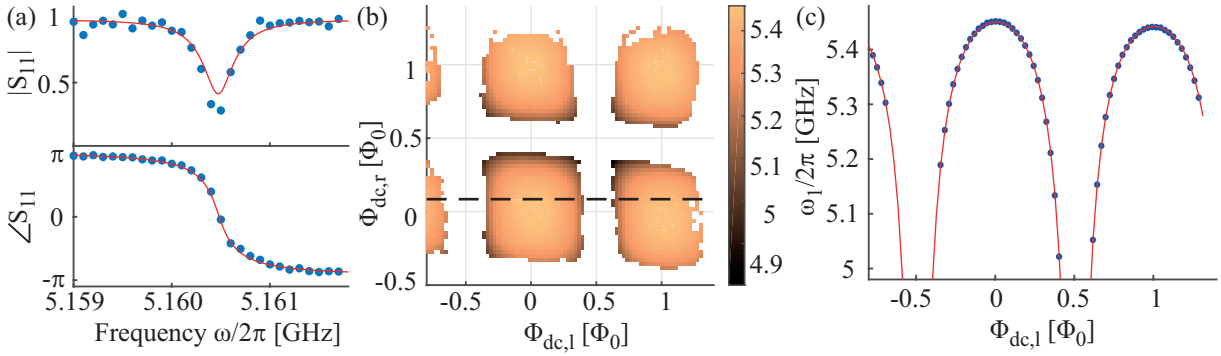

Figure 2. (a) Reflection measurement (blue dots) at $\Phi_{dc} = (0.3, 0.3)\,\Phi_0$ and a fit to the model $S_{11} = (1/Q_{ext} - 1/Q_{int} - 2i(\omega-\omega_1)/\omega_1)/(1/Q_{ext} + 1/Q_{int} + 2i(\omega-\omega_1)/\omega_1)$. For this bias point we can extract $\omega_1/2\pi = 5.1605\,\text{GHz}$, $Q_{ext} = 15.4 \cdot 10^3$ and $Q_{int} = 36.9 \cdot 10^3$. (b) dc tuning of the resonant frequency by both magnetic flux biases. (c) Linecut from (b) indicated by the black dashed line. The blue dots are data and the red line is a fit to the model in Eq. (1).

Table 1. Two-tone spectroscopy of the second resonator mode using parametric up-conversion. The first column indicates the flux bias point, ω_1 and ω_2 are the two lowest mode frequencies and the last column is the spectrum anharmonicity.

$(\Phi_{dc,l}, \Phi_{dc,r})$ [Φ_0]	$\omega_1/2\pi$ [GHz]	$\omega_2/2\pi$ [GHz]	$(2\omega_1 - \omega_2)/2\pi$ [MHz]
(0.01,0.01)	5.459	10.867	47
(0.21,-0.19)	5.360	10.668	52
(0.31,-0.29)	5.184	10.323	45

(Fig. 2(a)); the extracted resonant frequencies are presented in Fig. 2(b). The pattern is slightly tilted due to a small inductive crosstalk.

The second resonator mode is outside the frequency band of our setup, but its resonant frequency can be found using parametric up-conversion [22, 23], a two-photon process which we implement by letting a weak current-probe signal resonantly excite the first mode while simultaneously flux-pumping one of the SQUIDs at a lower frequency. When this pump tone hits the difference frequency $\omega_2 - \omega_1$, photons are up-converted from ω_1 to ω_2, resulting in an observed level-avoided crossing in the reflected signal, from which ω_2 can be determined. We list three measured points in Table 1. We conclude that the anharmonicity is much larger than the linewidth (2Γ) of the resonator. Importantly, this means that our pump tone, applied at frequency $2\omega_1$, should not excite the second harmonic.

By straightforward extension of the results in Ref. [10], the spectrum of the doubly tunable resonator is described by the equation

$$\frac{\omega_n}{v} d \tan\left(\frac{\omega_n}{v} d\right) \left[1 - \left(\frac{v}{\omega_n d}\right)^2 \left(\frac{1}{\gamma_l} - c\left(\frac{\omega_n}{v} d\right)^2\right)\left(\frac{1}{\gamma_r} - c\left(\frac{\omega_n}{v} d\right)^2\right)\right] = \frac{1}{\gamma_l} + \frac{1}{\gamma_r} - 2c\left(\frac{\omega_n}{v} d\right)^2. \tag{1}$$

The subscripts l/r correspond to the left and right SQUID, ω_n is the frequency of mode n, $d = 10.133\,\text{mm}$ is the resonator length and $v = 1/\sqrt{C_0 L_0}$ is the phase velocity. $\gamma_{l/r} = L_{J,l/r}/(L_0 d)$ is the inductive participation ratio, where the SQUID inductance is $L_{J,l/r} = \Phi_0/(2\pi I_c |\cos(\Phi_{dc,l/r}\pi/\Phi_0)|)$, assuming low signal levels, $I_s \ll I_c$, and $\Phi_{dc,l/r}$ is the static magnetic flux bias. The capacitive participation ratio is $c = C_J/C_0 d$. Here we have assumed that the two SQUIDs are nominally identical, $\gamma_0 = \gamma_{0,l} = \gamma_{0,r}$ and $C_J = C_{J,l} = C_{J,r}$.

The two-dimensional dc tuning, Fig. 2(b), together with the measurements of the second mode in Table 1, can be fitted using Eq. (1). A linecut of Fig. 2(b) with a fit is found in

Table 2. Extracted parameters for the resonator. The inductive participation ratio is $\gamma_0 = L_{J,0}/L_0 d$, I_c the SQUID critical current, C_J the SQUID capacitance and $\xi_{l/r}$ represents the dc-crosstalk. C_0 and L_0 are the capacitance and inductance per unit length of the coplanar waveguide. ω_1 is the resonant frequency of the lowest mode, Γ is the photon loss rate and Q_{int} and Q_{ext} are the quality factors of the resonator at $\Phi_{dc} = (0, 0)\,\Phi_0$. The translation between the loss rate Γ and the Q-values is $2\Gamma = \omega_1/Q_{\text{int}} + \omega_1/Q_{\text{ext}}$.

γ_0 [%]	I_c [μA]	C_J [fF]	ξ_l [%]	ξ_r [%]	C_0 [$\frac{\text{nF}}{\text{m}}$]	L_0 [$\frac{\mu\text{H}}{\text{m}}$]	$\omega_1(0)/(2\pi)$ [GHz]	$2\Gamma(0)/(2\pi)$ [MHz]	$Q_{\text{int}}(0)$ [10^3]	$Q_{\text{ext}}(0)$ [10^3]
4.64	1.64	89	3.64	4.19	0.159	0.427	5.459	0.56	400	9.6

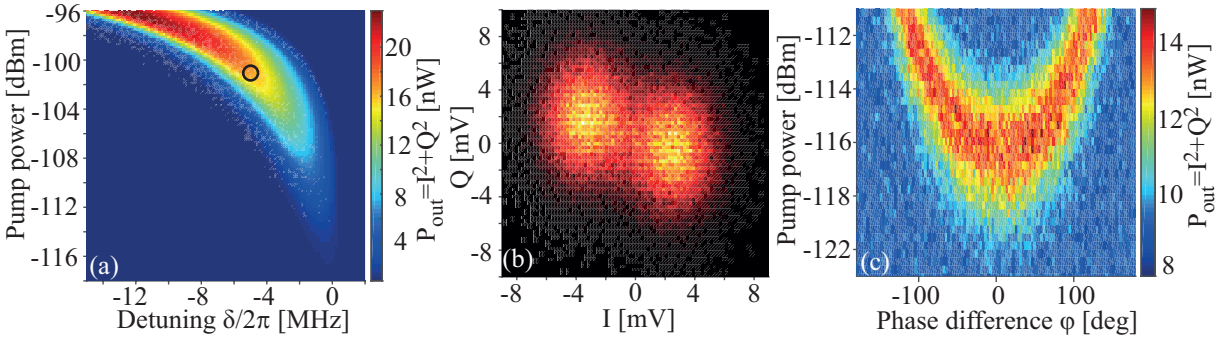

Figure 3. (a) Photon down-conversion, measured with a single pump applied to the left flux line at the bias point $(0.3, 0.3)\,\Phi_0$. (b) Histogram taken at the point marked with a black circle in (a). We measure two π-shifted states. (c) Double-pump measurement, where the phase difference φ between the pump signals is varied. Here the SQUID bias is $(0.2, 0.2)\,\Phi_0$ and $\delta = -1\,\text{MHz}$.

Fig. 2(c). Extracted resonator and SQUID parameters are found in Table 2. $\xi_{l/r}$ are the dc crosstalks, *i.e.* how much each SQUID is affected by the opposite flux line (only a few percent of the coupling from the closest flux line). The resonant frequency can be tuned over a wide frequency range: the limiting factor is the photon loss rate, which increases as $\Phi_{dc,l/r}$ approaches $\Phi_0/2$. However, as seen in Fig. 2(b), resonant frequencies below 4.9 GHz are measurable.

4. Measurement results - Pumping

By applying a pump tone to one of the ac flux lines at a frequency close to $2\omega_1$, we expect parametric oscillations at ω_1. We measure the quadrature components of the output signal, and calculate the total output power, $P_{out} = \langle I^2 \rangle + \langle Q^2 \rangle$. Fig. 3(a) shows photon down-conversion from $2\omega_1$ to ω_1 in a range of detuning and pump power. The detuning is denoted $\delta = \omega_p/2 - \omega_1$, where ω_p is the pump frequency. Furthermore, we sample the individual quadratures, $\langle I(t) \rangle$ and $\langle Q(t) \rangle$, and histogram $1 \cdot 10^5$ samples, see Fig. 3(b). The histogram shows two stable π-shifted states with the same amplitude, characteristic of parametric oscillations [8, 9, 24].

We can also apply pump signals to both flux lines simultaneously. The amplitudes are adjusted such that the effective pump strengths of the two individual SQUIDs are equal. This was done by measuring single-pump thresholds, which for the bias point $(0.2, 0.2)\,\Phi_0$ should be equal. We find that, depending on the phase difference $\varphi = \varphi_r - \varphi_l$, the threshold for photon generation changes, see Fig. 3(c).

The theoretical parametric oscillation threshold is $\epsilon_{th} = \sqrt{\Gamma^2 + \delta^2}$ both for the single and double pump cases. The measured oscillation regions are asymmetric in δ, due to a pump-induced frequency shift because of the resonator nonlinearity, shifting the resonant frequency

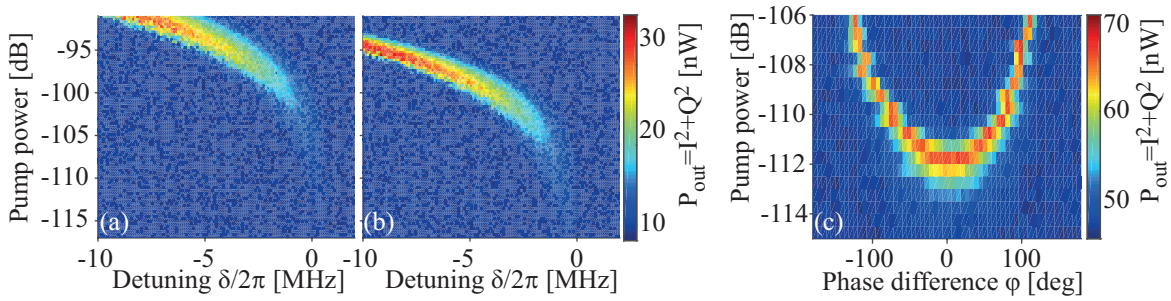

Figure 4. Measurement results at SQUID bias $(0, 0.2)\,\Phi_0$, in both cases using a single pump, coupled closest to the left (a), and the right (b) flux line respectively. (c) Double-pump measurement of a $\lambda/2$-resonator with only one SQUID, biased at $0.18\,\Phi_0$. Here $\delta = -6\,\mathrm{MHz}$.

towards red detuning. The threshold is reached at an effective pump strength $\epsilon_{eff} = \epsilon_{th}$. Following the formalism [10] and extending the results to the double pump case, the effective pump strength is a superposition of complex amplitudes of flux modulation in the left and right SQUIDs, $\Phi_{ac,l/r} = |\Phi_{ac,l/r}|e^{i\varphi_{l/r}}$, so that $\epsilon_{eff} = A(\omega_1)(k_l\Phi_{ac,l} + k_r\Phi_{ac,r})$. The coefficients are, $k_{l/r} = |\tan(\Phi_{dc,l/r}\pi/\Phi_0)|/\gamma_{l/r}$. This gives an expected minimum threshold and therefore maximum photon generation in the breathing mode, $\varphi = 0°$, but cancellation and consequently no photons in the vibrating mode, $\varphi = \pm 180°$, in agreement with the measured data.

5. Discussion

We find qualitative agreement between Fig. 3 and the doubly flux-pumped resonator theory as well as some interesting deviations. In Fig. 4(a) and (b), we present regions of photon down-conversion, at the bias point $(0, 0.2)\,\Phi_0$. A single pump tone is applied to the left flux line in (a) and to the right in (b). Since for (a) the pumping is around zero flux and in (b) around $0.2\,\Phi_0$, different results are expected. However, the shapes of the oscillation regions in the two graphs are rather similar, although the thresholds differ by around 5 dB. Setup attenuation differences cannot explain this large number. The observation of parametric oscillations at zero flux bias is surprising, since this contradicts theoretical predictions [10]. We attribute this effect to a possible strong inductive ac crosstalk or a parasitic coupling. Even though the crosstalk at dc is negligible, it could be large at microwave frequencies, due to differences in signal distribution on the chip for dc and microwave signals. In Fig. 4(a), the pump power applied to the left pump line would actually also pump the right SQUID, with a pump power leakage of 5 dB. Assuming that the ac flux is proportional to the pump amplitude, *i.e.* $\Phi_{ac} \propto 10^{(P_{pump})/20}$, this corresponds to 56 % crosstalk.

A parasitic coupling from the flux pump to the SQUID current could occur, due to the presence of the low impedance loop through the resonator center conductor and the ground plane. This loop is ~ 4000 times larger than the SQUID loop, which corresponds to a significantly larger inductance. A coupling to this loop could cause circulating currents, and thereby directly drive the SQUID current. A possible solution, making the loop less parasitic, would be to increase its impedance by changing the geometry of the gold-bridge and slot.

Another issue is the threshold pump strength. In experiments with a $\lambda/4$-resonator with identical SQUID flux-line design and similar resonant frequency, the single pump threshold is at least 20 dB higher than what is measured here. The length difference of a $\lambda/2$ and $\lambda/4$-resonator could account for maximum a few dB of difference. Therefore the differing thresholds have to be explained, either by differing pumping mechanisms or significantly differing flux line to SQUID coupling. However, the latter can be ruled out since the couplings are designed to be identical.

To find an explanation of the mentioned discrepancies, we performed a control experiment to probe the ac crosstalk. A similar resonator was fabricated with only one SQUID, *i.e.*, the other end was shorted to ground. Both resonator ends were equipped with on-chip flux lines, to allow for double-pump experiments. Surprisingly, we observe the same qualitative behaviour, independently of whether the resonator has two (Fig. 3(c)) or one (Fig. 4(c)) SQUID. There are some differences in output power and oscillation region widths, but this is because the measurements were performed with different samples, and at different bias points and detunings. This suggests an additional mechanism of down-conversion, possibly related to the microwave field filling the cavity and producing a current-pumping effect [25] such as that used in many parametric amplifiers [11, 26]. The difference between flux and current pumping has been discussed in Ref. [24]. The phase dependence of the threshold in Fig. 4(c), could, for instance, be explained by direct interference of the two pump signals.

6. Conclusion

Using a $\lambda/2$ resonator with two magnetic-flux-tunable boundary conditions, we demonstrated photon generation by degenerate downconversion of a pump tone. When pumping with two signals at the same frequency, we observed a pump-phase dependence of the instability threshold for photon generation. This is in agreement with a theoretical model for modulation of the boundary conditions. We also observed non-ideal results attributable to ac crosstalk and parasitic couplings resulting in current driving of the SQUIDs.

Acknowledgements

The authors acknowledge financial support from the European Research Council, the European project PROMISCE, the Swedish Research Council and the Wallenberg Foundation. J.B. acknowledges partial support by the EU under REA grant agreement no. CIG-618353.

References

[1] Casimir H B G 1948 *P. Roy. Neth. Acad. Arts Sci.* 793
[2] Moore G T 1970 *J. Math. Phys.* **11** 2679
[3] DeWitt B S 1975 *Phys. Rep.* **19** 295
[4] Fulling S A and Davies P C W 1976 *P. Roy. Soc. Lond. A Mat.* **348**
[5] Sandberg M *et al.* 2008 *Appl. Phys. Lett.* **92** 203501
[6] Johansson J R, Johansson G, Wilson C M and Nori F 2010 *Phys. Rev. A* **82** 052509
[7] Wilson C M *et al.* 2011 *Nature* **479** 376
[8] Dykman M I, Maloney C M, Smelyanskiy V N and Silverstein M 1998 *Phys. Rev. E* **57** 5202
[9] Wilson C M, Duty T, Sandberg M, Persson F, Shumeiko V and Delsing P 2010 *Phys. Rev. Lett.* **105** 233907
[10] Wustmann W and Shumeiko V 2013 *Phys. Rev. B* **87**(18) 184501
[11] Castellanos-Beltran M A and Lehnert K W 2007 *Appl. Phys. Lett.* **91** 083509
[12] Tholén E A *et al.* 2007 *Appl. Phys. Lett.* **90** 253509
[13] Yamamoto T *et al.* 2008 *Appl. Phys. Lett.* **93** 042510
[14] Roch N *et al.* 2012 *Phys. Rev. Lett.* **108**(14) 147701
[15] Lambrecht A, Jaekel M T and Reynaud S 1996 *Phys. Rev. Lett.* **77**(4) 615–618
[16] Ji J Y, Jung H H and Soh K S 1998 *Phys. Rev. A* **57** 4952
[17] Dodonov V V 1998 *J. Phys. A-Math. Gen.* **31** 9835
[18] Lambrecht A, Jaekel M T and Reynaud S 1998 *Eur. Phys. J. D* **3**(1)
[19] Dalvit D A R and Mazzitelli F D 1999 *Phys. Rev. A* **59** 3049
[20] Lindkvist J *et al.* 2014 *Phys. Rev. A* **90** 052113
[21] Bruschi D E, Sabín C, Kok P, Johansson G, Delsing P and Fuentes I 2016 *Sci. Rep.* **6** 18349
[22] Zakka-Bajjani E, Nguyen F, Lee M, Vale L R, Simmonds R W and Aumentado J 2011 *Nat. Phys.* **7**(8) 599
[23] Wustmann W and Shumeiko V 2017 *arXiv:1704.05083*
[24] Krantz P *et al.* 2016 *Nat. Commun.* **7** 11417
[25] Yurke B *et al.* 1988 *Phys. Rev. Lett.* **60**(9) 764
[26] Siddiqi I *et al.* 2005 *Phys. Rev. Lett.* **94**(2) 027005